

which the scattering is entirely due to lattice vibrations.² In the analysis of a number of samples with lattice scattering only, he found it necessary to multiply by a factor of 3.2 to obtain agreement of this exact theory with experiment. Comparison of the lattice scattering part of the 20° data with this theory shows about the same discrepancy.

Since the value of the mobility could not be incorrect by such a factor, this disagreement would seem to indicate that the rate of energy loss in collisions is higher than the previous considerations indicate by a factor of about nine. This could be the case, as Shockley points out, if the edge of the conduction band were degenerate. This would give rise to complex energy surfaces, which might give more effective energy dissipation for the electrons without affecting their mobility.

The imperfect fit in the region of sharp ascent can be ascribed to two factors: (1) the crude theoretical treatment, and (2) nonuniformity of the field in the sample because of variations in impurity concentration and cross section. It is also observed that at the very highest fields obtained, the experimental points fall below the line of slope $\frac{1}{2}$. This is expected if equipartition ceases to be valid for the lattice oscillators which scatter the electron, as can be seen from the following considerations. The probability of scattering of an electron by a particular mode of lattice vibration is proportional to the dilatation or deformation produced by the mode, which is in turn proportional to its energy. As the electron gets faster, it interacts with

shorter lattice waves. Under equipartition, fast electrons see no bigger deformation than slow ones, and the mean free path is independent of electron velocity. When the energy of the lattice oscillators is essentially the zero point energy, however, faster electrons see a more deformed lattice, and this leads to a mean free path which decreases with v or x , and a mobility which decreases more rapidly than $1/v$ or $1/x$. At the field intensity for which the departure from the line of slope $\frac{1}{2}$ becomes evident, the electron speed has been multiplied by a factor of about 6. If the effective mass of the electron were the free electron mass, the departure from equipartition should occur at much lower fields. An electron of smaller effective mass, however, would have smaller momentum for the same energy, and therefore interact with phonons of smaller energy. To account for the validity of equipartition out to the high fields observed, the effective mass would have to be of the order of one-sixth the mass of a free electron, which is in fair agreement with the previously stated value.

It can be concluded that a combination of scattering by ionized impurities and lattice vibrations accounts semiquantitatively for the variation of mobility with field that has been observed by Ryder. It is quite satisfactory, in the present state of the theory, that application of a theory assuming spherical energy surfaces to this case shows the same discrepancy as it does in the case where only lattice scattering is present.

I am indebted to Dr. W. Shockley for a number of valuable discussions on this subject.

Surface Barrier Analysis for the Highly Refractory Metals by Means of Schottky Deviations*

D. W. JÜENKER, G. S. COLLADAY,† AND E. A. COOMES
University of Notre Dame, Notre Dame, Indiana

(Received February 5, 1953)

The theory for the deviation from the Schottky effect is redeveloped for the thermionic case, using the Herring and Nichols coefficients μ and λ , which are typical of the two reflection regions of the metallic surface barrier. The assumptions of Guth and Mullin are used, but correction of their calculations leads to new results; a method of data analysis based on these results is described. In this method the Guth-Mullin assumptions regarding the form of the barrier are taken as a first approximation to the real case. The method is applied to available experimental data on tungsten, tantalum, and molybdenum. One may draw the following conclusions: The outer (λ) reflection region behaves in accordance with the mirror-image law, while the innermost (μ) is field-independent. The phase change suffered by an electron wave crossing the μ -region is less than that computed for the theoretical box model. All three metals studied are mutually similar as regards the potential form in the μ -region. Apparently, it is not yet possible to evaluate the zero-field reflection coefficient from deviation amplitudes; this is probably due to the parabolic approximation used for the λ -region in the theory.

I. INTRODUCTION

THE phenomenon of periodic deviations from the Schottky effect¹⁻³ has been accounted for by

Guth and Mullin⁴ in terms of the interference between electron waves reflected from the emitter surface and the region of the barrier maximum. Herring and

* This research was sponsored by the U. S. Navy Bureau of Ships.

† Now at the U. S. Naval Ordnance Test Station, Inyokern, California.

¹ R. L. E. Seifert and T. E. Phipps, *Phys. Rev.* **56**, 652 (1939).

² D. Turnbull and T. E. Phipps, *Phys. Rev.* **56**, 663 (1939).

³ Munick, LaBerge, and Coomes, *Phys. Rev.* **80**, 887 (1950).

⁴ E. Guth and C. J. Mullin, *Phys. Rev.* **59**, 575 (1941).

Nichols⁵ have suggested the utility of this effect in the study of emitter surfaces and have outlined a device for analyzing experimental data. This method is based on an assumption implicit in the theory of Guth and Mullin that the regions of the surface barrier responsible for electron reflections do not overlap appreciably. Therefore, one may define two complex reflection coefficients, μ and λ , applicable to the de Broglie waves impinging on the surface and on the barrier maximum, respectively. Presentation of a theory for the Schottky deviation in terms of μ and λ is advantageous in that the physical significance of such measurable quantities as period, phase, and amplitude becomes apparent, and a clear interpretation of experimental data can be made.

The present work purposes to formulate deviation theory in a more useful form and then to separate from existing data on the highly refractory metals various properties of their surface barriers. The theory has been redeveloped on the basis of a double reflection effect, using the Herring and Nichols coefficients together with the general assumptions of Guth and Mullin regarding the form of the potential near the barrier maximum and the validity of the WKB approximation between the two reflection points.

II. THEORY

A. Box Model Transmission Coefficient

In the following development, four major assumptions are used:

(a) The barrier outside a clean metal surface is of the mirror-image type (Fig. 1).

(b) The point x_1 at which the image potential joins the interior potential is close to the surface, such that the reflections in this region are independent of applied field. Those reflections at x_1 which contribute to Schottky deviations should be practically independent of electron energy as well.

(c) In the region extending from x_1 to a short distance to the left of the barrier maximum x_0 , the WKB approximation is valid for electrons taking part in the deviation effect. That is, in this region the probability for electron reflection is small.

(d) The surface barrier has a parabolic shape in the vicinity of x_0 ; also, there exists to the left of x_0 a region where the parabolic approximation and the WKB approximation are simultaneously valid.

Assumption (a) may be stated:

$$V = -(2x)^{-1} - x(2x_0^2)^{-1}, \text{ for } x \geq x_1, \quad (1a)$$

where V is the potential energy of an electron, relative to infinity, at a distance x from the surface. The quantities x and x_0 are in units of the first Bohr radius ($a_0 = \hbar^2/m_e e_2 = 0.529A$), and x_0 is the position of the barrier maximum, given by

$$x_0 = 3.587 \times 10^4 E^{-1/2}.$$

⁵ C. Herring and M. H. Nichols, Revs. Modern Phys. 21, 185 (1949), Chap. 4.

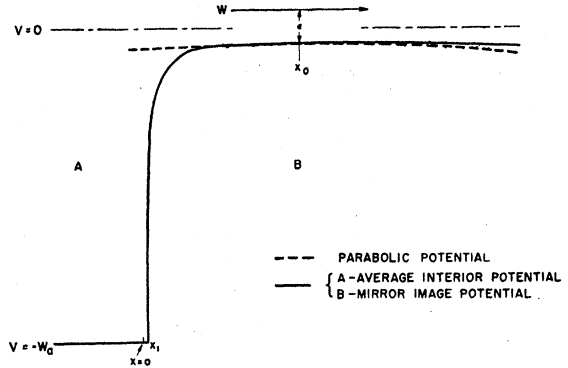


FIG. 1. The metallic surface barrier. The electronic potential energy V , measured relative to infinity, is plotted as a function of distance x from the surface of the emitter for the case of the box model. The form shown in region B is due to mirror-image plus applied field. At x_1 , this joins the average interior potential $-W_0$, shown in region A . The dashed line indicates the parabolic approximation near the barrier maximum x_0 . The energy of the emitted electron is $W = \epsilon + V(x_0)$.

Here E is the applied field in volt-cm⁻¹, and V is in units of the ionization potential of hydrogen ($W_H = me^4/2\hbar^2 = 13.58$ ev).

For the box model, as shown in Fig. 1, the potential to the left of x_1 is constant:

$$V = -W_0, \text{ for } x \leq x_1. \quad (1b)$$

Thus, from (1a) and (1b), the position of x_1 is found to a good approximation to be $x_1 = (2W_0)^{-1}$. Potentials (1a) and (1b) are shown in regions B and A , respectively, in Fig. 1.

In region B , the wave number of an electron whose energy is $W = \epsilon + V(x_0)$ is

$$\kappa_B = (W - V)^{1/2} = [\epsilon + (x_0 - x)^2(2xx_0^2)^{-1}]^{1/2}. \quad (2a)$$

For small ϵ , and in region A ,

$$\kappa_A \simeq (2x_1)^{-1/2} = W_0^{1/2}. \quad (2b)$$

Following Guth and Mullin,⁴ one can express the wave functions to the left of x_1 and between x_1 and x_0 as a plane wave and a first-order WKB wave. That is,

$$\psi_A = a_1 \exp(i\kappa_A x) + a_2 \exp(-i\kappa_A x), \text{ for } x \leq x_1 \quad (3a)$$

and

$$\psi_B = b_1 \kappa_B^{-1/2} \exp\left(i \int_{x_0}^x \kappa_B dx\right) + b_2 \kappa_B^{-1/2} \exp\left(-i \int_{x_0}^x \kappa_B dx\right), \text{ for } x_1 \leq x < x_0. \quad (3b)$$

By joining ψ_A to ψ_B at x_1 , one can find a complex reflection coefficient μ_0 characteristic of x_1 . Letting $b_2 = 0$,

$$\mu_0 = (a_2/a_1)_{b_2=0} = \rho(1 + \rho^2)^{-1/2} \exp[i(\pi/2 + 2\kappa_1 x_1 + \tan^{-1}\rho)], \quad (4)$$

where

$$\rho = |\kappa_1'/4\kappa_1^2|, \quad \kappa_1 = \kappa_B(x_1) = \kappa_A = W_a^{\frac{1}{2}}, \\ \kappa_1' = (d\kappa_B/dx)_{x_1} = -W_a^{\frac{1}{2}}.$$

It will also prove useful to evaluate two complex transmission coefficients for x_1 , namely, $t_1 = (b_1/a_1)_{b_2=0}$ and $t_2 = (a_2/b_2)_{a_1=0}$. The arguments of these coefficients are found to be given by

$$\arg t_1 = \arg t_2 = \kappa_1 x_1 - \int_{x_0}^{x_1} \kappa_B dx + \tan^{-1} \rho. \quad (5)$$

A coefficient similar to μ_0 may be defined in the neighborhood of x_0 :

$$\lambda_0 = b_2/b_1,$$

where b_1 and b_2 are so chosen that an electron wave at $x = \infty$ is purely outgoing. Such a choice has been made by Guth and Mullin,⁴ who deduce b_1 and b_2 by joining (3b) to the parabolic cylinder solution for the wave equation in the immediate vicinity of x_0 . The correct asymptotic expansion for the parabolic function, as taken from their work, has the form:⁶⁻⁹

$$\psi_p \propto z^{-\frac{1}{2}} [(2\pi)^{\frac{1}{2}}/\Gamma(\frac{1}{2} - i\beta\epsilon)] \\ \times \exp[-\pi\beta\epsilon/4 - i(z^2/4 + \beta\epsilon \ln z - \pi/8)] \\ + z^{-\frac{1}{2}} \exp[-3\pi\beta\epsilon/4 + i(z^2/4 + \beta\epsilon \ln z - 3\pi/8)], \quad (6)$$

where $\beta = (x_0^2/2)^{\frac{1}{2}}$, ϵ is the electron energy relative to the barrier top, and $z = (x_0 - x)/\beta^{\frac{1}{2}}$. The two terms in this function represent the outgoing and incoming waves, respectively, to the left of x_0 . The ratio of these terms should be equal to the corresponding ratio of the two parts of (3b) at some value of x where the potential is parabolic and the WKB approximation valid. Approximating $z^2 \gg 4|\beta\epsilon|$ at this point, the value of λ_0 corresponding to this joining condition is

$$\lambda_0 = b_2/b_1 \simeq (2\pi)^{-\frac{1}{2}} \Gamma(\frac{1}{2} - i\beta\epsilon) \\ \times \exp[-\pi\beta\epsilon/2 + i(\beta\epsilon \ln \beta\epsilon - \pi/2)].$$

Since $|\Gamma(\frac{1}{2} - i\beta\epsilon)| = (2\pi)^{\frac{1}{2}} e^{\pi\beta\epsilon/2} (1 + e^{2\pi\beta\epsilon})^{-\frac{1}{2}}$, one can make the approximation that $\arg \Gamma(\frac{1}{2} - i\beta\epsilon) \simeq C\beta\epsilon$, where $C = (\gamma_E + 2 \ln 2) = 1.96$ and $\gamma_E = 0.56$ (Euler's constant). Therefore,

$$\lambda_0 = (1 + e^{2\pi\beta\epsilon})^{-\frac{1}{2}} \exp[i(C + \ln \beta\epsilon)\beta\epsilon - i\pi/2]. \quad (7)$$

Now the particle transmission coefficient for the entire barrier may be written in the form suggested by Herring and Nichols,⁵ namely,

$$D = 1 - R = 1 - |(\lambda + \mu)/(1 + \mu^*\lambda)|^2,$$

in which

$$\mu = \mu_0 \quad (8a)$$

⁶ E. Guth and C. J. Mullin employ that form of the parabolic function which evolves into an incoming wave at $x = \infty$. While this gives qualitatively correct results, it introduces an error in the phase of the periodic deviation. An alternate form of the function, which they also quote, provides the correct outgoing wave for large x , and is used here.

⁷ E. Guth and C. J. Mullin, Phys. Rev. **59**, 867 (1941).

⁸ E. Guth and C. J. Mullin, Phys. Rev. **60**, 535 (1941).

⁹ E. Guth and C. J. Mullin, Phys. Rev. **61**, 339 (1942).

and

$$\lambda = \lambda_0 \exp[i(\arg t_1 + \arg t_2)]. \quad (8b)$$

The exponential terms in (8b) embody the phase accumulation of an electron wave proceeding from the left of x_1 to x_0 and returning, excepting that phase change occurring in the reflection at x_0 . This latter is contained in the argument of λ_0 . Expanding D and neglecting terms in $|\mu|$ of order higher than two, one gets

$$D = D_0 + D_1 + D_2, \quad (9a)$$

where

$$D_0 = 1 - |\lambda|^2, \quad (9b)$$

$$D_1 = -|\mu|^2 [(1 - |\lambda|^2)^2 - 2|\lambda|^2(1 - |\lambda|^2) \cos 2\sigma], \quad (9c)$$

$$D_2 = 2|\mu| |\lambda| (1 - |\lambda|^2) \cos \sigma, \quad (9d)$$

and

$$\sigma = \arg \lambda - \arg \mu + \pi. \quad (9e)$$

B. Average Nonperiodic Transmission Coefficient

While the transmission coefficient given in (9) is independent of the mechanism for emission, the present treatment will be limited to the thermionic case. Accordingly, the average of D over a Maxwellian distribution of energies will be computed. Designating this average as $\langle D \rangle_{Av}$,

$$\langle D \rangle_{Av} \equiv \int_{-\infty}^{\infty} D(\epsilon) e^{-\epsilon/kT} d\epsilon / \int_0^{\infty} e^{-\epsilon/kT} d\epsilon.$$

The dominant periodic term D_2 (9d) is of principal interest, but for the sake of completeness the calculations for $\langle D_0 \rangle_{Av}$ and $\langle D_1 \rangle_{Av}$ are included. Let us introduce the variable $\alpha = |\beta\epsilon|$, and the quantity $B = (2\pi\beta kT)^{-1}$, where β is given in (6) and T is the absolute temperature. Then, from (7), (8), and (9), D_0 may be stated in the form

$$D_0 = \begin{cases} 1 - \sum_{n=1}^{\infty} (-1)^{n+1} e^{-n2\pi\alpha}, & \text{for } \epsilon > 0, \\ \sum_{n=1}^{\infty} (-1)^{n+1} e^{-n2\pi\alpha}, & \text{for } \epsilon < 0. \end{cases}$$

The average is

$$\langle D_0 \rangle_{Av} = 1 - 2\pi B \sum_{n=1}^{\infty} (-1)^{n+1} \\ \times \left\{ \int_0^{\infty} \exp[-n2\pi(1+B/n)\alpha] d\alpha \right. \\ \left. + \int_0^{\infty} \exp[-n2\pi(1-B/n)\alpha] d\alpha \right\} \\ = 1 + 2B^2 \sum_{n=1}^{\infty} (-1)^{n+1} n^{-2} [1 - (B/n)^2]^{-1}. \quad (10a)$$

Similarly, since $|\mu|$ may be considered energy-independent, the nonperiodic part of D_1 and its average are

$$D_1(m) = \begin{cases} -|\mu|^2 \left[1 - \sum_{n=1}^{\infty} (-1)^{n+1} (n+1) e^{-n2\pi\alpha} \right], & \text{for } \epsilon > 0, \\ |\mu|^2 \sum_{n=1}^{\infty} (-1)^{n+1} (n-1) e^{-n2\pi\alpha}, & \text{for } \epsilon < 0, \end{cases}$$

and

$$\langle D_1(m) \rangle_{Av} = -|\mu|^2 \left\{ 1 - 2B \sum_{n=1}^{\infty} (-1)^{n+1} \times [1 - B/n^2][1 - B^2/n^2]^{-1} \right\}. \quad (10b)$$

For positive or negative energies, the amplitude of the periodic part of D_1 is

$$|D_1(p)| = 2|\mu|^2 \sum_{n=1}^{\infty} (-1)^{n+1} n e^{-n2\pi\alpha}.$$

The average of this quantity exceeds the amplitude of $\langle D_1(p) \rangle_{Av}$:

$$|\langle D_1(p) \rangle_{Av}| < \langle |D_1(p)| \rangle_{Av} < 4|\mu|^2 B \sum_{n=1}^{\infty} (-1)^{n+1} [1 - B^2/n^2]^{-1}. \quad (10c)$$

C. Average Periodic Transmission Coefficient

Using (4), (5), (7), and (8), the statement of (9e) becomes

$$\sigma = 2 \int_{x_1}^{x_0} \kappa_B dx + \tan^{-1} \rho + (C + \ln \beta \epsilon) \beta \epsilon. \quad (11)$$

The phase integral in the first term on the right may be written

$$\int_{x_1}^{x_0} \kappa_B dx = \int_{x_1}^{x_0} \kappa_0 dx + f(\epsilon),$$

where $\kappa_0 = (x_0 - x) / (2xx_0^2)^{1/2}$, and κ_B is given in (2a). Numerical integration shows that $f(\epsilon)$ can be represented approximately by

$$\text{Re } f(\epsilon) = \text{Re} \int_{x_1}^{x_0} (\kappa_B - \kappa_0) dx \simeq 1.5 |\beta \epsilon|^{-0.2} \beta \epsilon.$$

For the case of tunneling ($\epsilon < 0$), $f(\epsilon)$ has also an imaginary part which is cancelled by the imaginary contribution of the logarithmic term in (11). Thus, (11) becomes

$$\sigma = \sigma_0 \pm \sigma_1(\alpha), \quad (12a)$$

where

$$\sigma_0 = 2 \int_{x_1}^{x_0} \kappa_0 dx + \tan^{-1} \rho \simeq (4\sqrt{2}/3) x_0^{1/2} - 2W_a^{-1/2} + W_a^{1/2}/4, \quad (12b)$$

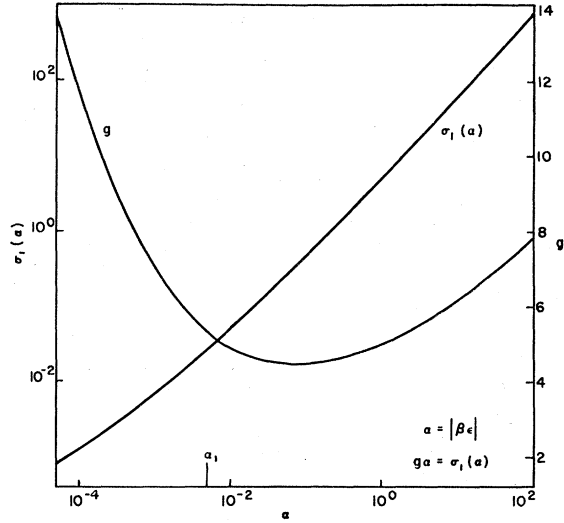


FIG. 2. The energy-dependent phase $\sigma_1(\alpha)$ of the unaveraged periodic transmission coefficient D_2 . Here σ_1 approaches zero with decreasing values of $\alpha = |\beta \epsilon|$ and is nearly directly proportional to α over the range effective in contributing to the deviation effect ($\alpha_1 < \alpha < 1$). The constant g of this proportionality is also plotted as a function of α .

and

$$\sigma_1(\alpha) = (C + \ln \alpha + 3.0 \alpha^{-1/5}) \alpha, \quad (12c)$$

and where α is again used to denote $|\beta \epsilon|$.

From (7) and (9), the amplitude of D_2 is

$$|D_2| = \begin{cases} 2|\mu| \sum_{n=0}^{\infty} (-1)^n \frac{\Gamma(n + \frac{3}{2})}{\Gamma(\frac{3}{2})\Gamma(n+1)} e^{-(n+\frac{1}{2})2\pi\alpha}, & \text{for } \epsilon > 0, \\ 2|\mu| \sum_{n=0}^{\infty} (-1)^n \frac{\Gamma(n + \frac{3}{2})}{\Gamma(\frac{3}{2})\Gamma(n+1)} e^{-(n+1)2\pi\alpha}, & \text{for } \epsilon < 0. \end{cases}$$

In order to average the combination of this with $\cos \sigma$, one must compute the integral:

$$I_n = \int_0^{\infty} e^{-a_n \alpha} \cos[\sigma_0 \pm \sigma_1(\alpha)] d\alpha, \quad (13)$$

where a_n is $2\pi[(n + \frac{1}{2}) + B]$ for $\epsilon > 0$ and $2\pi[(n+1) - B]$ for $\epsilon < 0$. Anticipating the high temperature approximation to be discussed in the following section, one may neglect the term B in a_n , leaving

$$a_n = \begin{cases} 2\pi(n + \frac{1}{2}), & \text{for } \epsilon > 0, \\ 2\pi(n+1), & \text{for } \epsilon < 0. \end{cases}$$

Also, consideration of the function $\sigma_1(\alpha)$, as given in (12) and graphed in Fig. 2, shows that for $\alpha < \alpha_1 = 5 \times 10^{-3}$, σ_1 is so small that its cosine may be replaced by unity and its sine by σ_1 itself. From (13), it is seen that for $\alpha > 1$, the integrand becomes negligible. In the intermediate region, where $\alpha_1 < \alpha < 1$, σ_1 may be considered the linear function of α , $\sigma_1 = g\alpha$. The factor g , which is also plotted in Fig. 2, has a value between 4.4

and 5.3 in the region of interest. Therefore, the integral in (13) may be expressed as

$$I_n = (J_0 + J_1) \cos \sigma_0 - (J_2 + J_3) \sin \sigma_0. \quad (14)$$

Using $G_n = g/a_n$, and defining an average $\sigma_1(\alpha)$ by the relation

$$\langle \sigma_1(\alpha_1) \rangle_{Av} = \int_0^{\alpha_1} \sigma_1(\alpha) e^{-a_n \alpha} d\alpha / \int_0^{\alpha_1} e^{-a_n \alpha} d\alpha,$$

the various terms in (14) may be written:

$$J_0 = \int_0^{\alpha_1} e^{-a_n \alpha} d\alpha = a_n^{-1} (1 - e^{-a_n \alpha_1}).$$

$$J_1 = \int_{\alpha_1}^{\infty} e^{-a_n \alpha} \cos(g\alpha) d\alpha = a_n^{-1} e^{-a_n \alpha_1} \times [1 - G_n \sigma_1(\alpha_1)] [1 + G_n^2]^{-1},$$

$$J_2 = \pm \int_0^{\alpha_1} e^{-a_n \alpha} \sigma_1(\alpha) d\alpha = \pm a_n^{-1} \langle \sigma_1(\alpha_1) \rangle (1 - e^{-a_n \alpha_1}),$$

$$J_3 = \pm \int_{\alpha_1}^{\infty} e^{-a_n \alpha} \sin(g\alpha) d\alpha = \pm a_n^{-1} e^{-a_n \alpha_1} [G_n + \sigma_1(\alpha_1)] [1 + G_n^2]^{-1},$$

where the + and - correspond to the sign of ϵ , the excess energy of an electron at x_0 .

Considering the smallness of J_0 and J_2 , it appears that, in the average, not only large values of $\alpha = |\beta\epsilon|$, but very small values as well, are ineffective in producing the deviation effect. At least, this is the case when a parabolic approximation is used for the potential near x_0 , despite the fact that the contribution per electron is greatest for small α .

Now G_n is never greater than about $\frac{3}{2}$, and $\langle \sigma_1(\alpha_1) \rangle_{Av}$

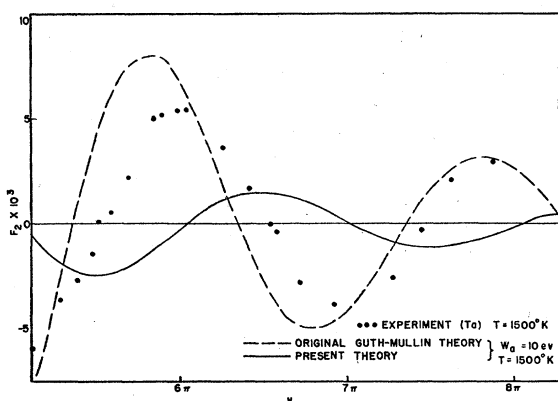


FIG. 3. The Schottky deviation F_2 , as a function of $y = 357.1/E^2$. The experimental points are for clean tantalum (see reference 3) at 1500°K and may be taken as typical of the data for the highly refractory metals. The dashed line represents the original Guth-Mullin theory (see reference 4), and the solid line is a plot of the theory developed in the text.

$\langle \sigma_1(\alpha_1) \rangle \ll 1$, so that (14) may be rewritten

$$I_n(\pm) = a_n^{-1} [1 - e^{-a_n \alpha_1} G_n^2 (1 + G_n^2)^{-1}] \cos \sigma_0 \mp a_n^{-1} [e^{-a_n \alpha_1} G_n (1 + G_n^2)^{-1}] \sin \sigma_0. \quad (15)$$

Replacing this in D_2 , the average of the latter may be written

$$\langle D_2 \rangle_{Av} = 4\pi |\mu| B \sum_{n=0}^{\infty} (-1)^n \frac{\Gamma(n + \frac{3}{2})}{\Gamma(\frac{3}{2}) \Gamma(n+1)} \times [I_n(+) + I_n(-)], \quad (16)$$

where $B = (2\pi\beta kT)^{-1}$, as before, and where $I_n(+)$ and $I_n(-)$ represent (15) evaluated for $\epsilon > 0$ and $\epsilon < 0$, respectively. It has been indicated previously that the value of g to be used in evaluating $G_n = g/a_n$ lies between 4.4 and 5.3. If the summation in (16) is performed numerically for each of these limiting values, the phases of the resultant expressions are found to differ by a small amount, about 0.1 radian; the amplitudes differ by 25 percent. Probably the most suitable value of g is close to that for lowest energy, namely 5.3. In this case,

$$\langle D_2 \rangle_{Av} = 0.96 |\mu| B \cos(\sigma_0 + 0.6). \quad (17a)$$

D. High Temperature Approximation

The modulus $|\mu|$ of the surface reflection coefficient given in (4) has a value of about 0.2 for a typical metal whose W_a value is 10 eV. The quantity $B = (2\pi\beta kT)^{-1}$ is about 0.1 for a field of 5×10^5 volt-cm $^{-1}$ and a temperature of 1000°K. It appears to be justified, therefore, to discard all terms in (10) smaller than $|\mu|B$ or B^2 . The remainders are

$$\langle D_0 \rangle_{Av} = 1 + (\pi B)^2 / 12 \quad (17b)$$

and

$$\langle D_1 \rangle_{Av} = -|\mu|^2. \quad (17c)$$

Equation (17a) gives the value of the periodic term $\langle D_2 \rangle$ after the high temperature approximation has been applied.

The total average transmission coefficient may be written, using Eq. (17):

$$\langle D(B) \rangle_{Av} = \langle D(0) \rangle_{Av} + (\pi B)^2 / 12 + 0.96 |\mu| B \cos(\sigma_0 + 0.6), \quad (18)$$

where $\langle D(0) \rangle_{Av} = 1 - |\mu|^2$ is the zero-field ($B=0$) transmission coefficient and σ_0 is given by (12b).

$\langle D(B) \rangle_{Av}$ is more useful when written in terms of the current, as a part of the Schottky relation

$$\log(I/I_0) = mE^{\frac{3}{2}} + \log \langle D(B) \rangle_{Av} - \log \langle D(0) \rangle_{Av},$$

where m is the Schottky slope and E the applied field. The last two terms on the right constitute the deviation from the Schottky effect and are made up of a monotonic and a periodic function of field, which have been

TABLE I. Analysis of the experimental Schottky deviation phase for tungsten, tantalum, and molybdenum. The position of the extremum in radians is y_m as given by Eq. (21a). Maxima are italicized. The mean separation of successive extrema is $\langle \Delta y \rangle_{Av}$ given theoretically by $\langle \Delta y \rangle_c = \pi = 3.1$. The mean experimental phase $\langle \delta_x \rangle_{Av}$ [Eq. (21b)] is quoted for each set of data, the box model value being indicated by δ_c , which is computed from Eq. (20b) for the W_a values shown. Asterisks designate mechanically polished samples.

	Tungsten ($W_a = 10.3$ ev)				Tantalum ($W_a = 9.3$ ev)			Molybdenum ($W_a = 10.2$ ev)	
	Seifert, Phipps ^a	Turnbull, Phipps ^b	Nottingham ^c *	Houde ^d	Seifert, Phipps ^a	Munick, LaBerge, Coomes ^e	Finn, LaBerge, Coomes ^f *	Brock, Houde, Coomes ^g	Haas ^h *
y_m , for $m=4$		<i>13.0</i>							
5	16.0	15.9	15.9	15.8				17.0	
6	<i>18.7</i>	<i>19.2</i>	<i>19.2</i>	<i>19.2</i>	<i>19.0</i>	18.7		<i>19.6</i>	<i>19.5</i>
7	21.9	21.9	22.3		22.2	21.9		22.7	22.2
8	<i>25.3</i>	<i>25.3</i>	<i>25.3</i>		<i>25.3</i>	<i>24.9</i>	25.1	<i>25.6</i>	<i>25.3</i>
9		28.2	28.2		28.2	27.9	28.4	28.7	28.1
10		<i>31.3</i>				<i>31.1</i>			<i>31.3</i>
11		34.0							
$\langle \Delta y \rangle_{Av}$	3.1	3.0	3.1	3.4	3.1	3.1	3.3	2.9	3.0
$\langle \delta_x \rangle_{Av}$	2.1	2.1	2.3	2.3	2.2	1.9	2.2	2.8	2.3
δ_c			3.6			3.8		3.7	

^a Reference 1.

^b Reference 2.

^c Reference 10.

^d Reference 13.

^e Reference 3.

^f Reference 11.

^g Reference 12.

Reference 14.

called F_1 and F_2 , respectively.³ Thus,

$$F_1 + F_2 = \log \langle D(B) \rangle_{Av} - \log \langle D(0) \rangle_{Av} \\ = \log I - \log I_0 - mE^{\frac{1}{2}}. \quad (19a)$$

Using logarithms to the base ten and translating σ_0 and B into units consistent with field in volt-cm⁻¹ and temperature in deg K,

$$F_1 = 2.0 \times 10^{10} T^{-2} y^{-6}, \quad (19b)$$

$$F_2 = 9.2 \times 10^4 |\mu| T^{-1} y^{-3} \cos(y + 2.1 - \delta), \quad (19c)$$

where $y = 357.1/E^{\frac{1}{2}}$, and $|\mu|$ and δ have, for the box model, the values

$$|\mu|_c = 0.0679 W_a^{\frac{1}{2}}, \quad (20a)$$

$$\delta_c = \arg \mu_0 - \arg t_1 - \arg t_2 + y \\ = \pi/2 + 7.37/W_a^{\frac{1}{2}} - 0.0679 W_a^{\frac{1}{2}}, \quad (20b)$$

as given in Sec. IIA. The terms $|\mu|$ and δ have been set apart from the others, since they arise in the reflection and transmission coefficients given in (4) and (5) for the position x_1 . They therefore typify the potential form at the surface of the emitter. The form of F_2 , in (19c), does not depend on the box model for the surface potential, but only on the initial assumptions made in Sec. IIA.

The small monotonic deviation F_1 has never been conclusively observed. F_2 can be separated from experimental Schottky data¹⁻³ and can be plotted as a function of y , as in (19c), for purposes of analysis. A comparison of (19c) with the original theory of Guth and Mullin and with experiment is shown in Fig. 3.

It is to be noted that, if the period in y is found experimentally to be constant and equal to 2π and if the amplitude varies as y^{-3} , the assumptions regarding the mirror-image barrier and the field- and energy-independence of μ are probably well founded. This being

the case, values for $|\mu|$ and the phase factor δ may be calculated from available data.

III. EXPERIMENT

A. Data on the Highly Refractory Metals

The data to be considered in the following section have been drawn from the work of Seifert, Turnbull, and Phipps^{1,2} on tungsten and tantalum, of Nottingham¹⁰ on tungsten, of Munick, LaBerge, Finn, and Coomes^{3,11} on tantalum, and of Brock, Houde, and Coomes¹² on molybdenum. Some unpublished results on tungsten¹³ and molybdenum¹⁴ have also been included. Round filaments were used for all the work represented, and at least one set of results for each of the three metals was obtained from a mechanically polished filament.

Although the deviations found in some of the work were separated from their Schottky lines in regions not totally free of patch effect, it appears that such deviations are patch-sensitive in amplitude but not in period.^{3,12} This is borne out by the agreement between deviations taken from different samples of the same metal. The patch sensitivity of the amplitudes makes verification of their field- and temperature-dependence difficult and limits the type of data from which $|\mu|$ can be calculated [see Eq. (19c)]. Deviations taken from relatively patch-free data, such as that of Seifert and Phipps on 1-mil tungsten and of Munick, LaBerge, and Coomes on 1-mil tantalum, indicate the correct dependence for the amplitude. All results are in agreement on the temperature-independence of the phase and period.

¹⁰ W. B. Nottingham, Phys. Rev. **57**, 935 (1940).

¹¹ Finn, LaBerge, and Coomes, Phys. Rev. **81**, 889 (1951).

¹² Brock, Houde, and Coomes, Phys. Rev. **89**, 851 (1953).

¹³ A. L. Houde, Ph.D. dissertation, University of Notre Dame, 1952 (unpublished).

¹⁴ G. A. Haas, University of Notre Dame (unpublished).

TABLE II. Amplitude analysis for patch-free data on tungsten and tantalum, and for the best available data on molybdenum. Here y_m indicates the extrema analyzed; $|\mu|_x$ is computed from Eq. (21c). The largest and smallest values are given. The corresponding theoretical value $|\mu|_c$ is calculated for the box model, using the WKB wave function for $x \geq x_1$ and the W_a given in Table I.

	Tungsten Seifert, Phipps ^a	Tantalum Munick, LaBerge, Coomes ^b	Molybdenum Brock, Houde, Coomes ^c
y_m	21.9, 25.3	24.9, 27.9, 31.1	25.6, 28.7
$ \mu _x$	0.7-0.8	0.6-0.8	0.5-0.7
$ \mu _c$	0.2	0.2	0.2

^a Reference 1.

^b Reference 3.

^c Reference 12.

B. Data Analysis

The field position E_m of each deviation extremum can be converted to its corresponding value in the parameter y by

$$y_m = 357.1/E_m^{\frac{1}{2}}, \quad (21a)$$

where E is the applied field in volt-cm⁻¹. The experimental value of δ can then be found from

$$\delta_x = y_m - m\pi + 2.1, \quad (21b)$$

where $m\pi$ is the integral multiple of π closest to y_m , m being even for maxima, odd for minima. Then δ_x can be compared with the value δ_c computed for the box model from (20b), using $W_a = 10.3$ eV for tungsten, 9.3 eV for tantalum, and 10.2 eV for molybdenum. The results of these computations performed on the data for the highly refractory metals are shown in Table I.

Limits for the experimental value of $|\mu|$ have been calculated from the data cited in Table II, using

$$|\mu|_x = 1.09 \times 10^{-5} A T y_m^3, \quad (21c)$$

as derived from (19c). Here, A is the deviation amplitude at the position y_m of the m th extremum, and T is the absolute temperature. The extrema used in the table are those most free of patch difficulties. The box model values for $|\mu|$ were computed from (20a), using the W_a figures quoted in Table I.

IV. SUMMARY AND CONCLUSIONS

The results of the data analysis shown in Tables I and II may be summarized as follows:

- (1) The half-period of the deviations in the parameter y is equal to π within the limits of experimental error.
- (2) The magnitude of the deviation phase is less than that predicted on the basis of the box model by an amount of the order of a quarter period.
- (3) No conclusive difference exists between the phase characteristics of tungsten, tantalum, and molybdenum.
- (4) The values for $|\mu|$ computed from experimental

deviation amplitudes are, in general, about three times larger than those calculated for the box model.

The period of the deviations indicates that the mirror-image form is the correct one for the surface barrier, and that δ , which is a function of the conditions near the emitter surface, is not a function of applied field. This condition limits the region characterized by the reflection coefficient μ to a short, field-independent, distance from the surface.

The discrepancy between the experimental δ_x and the box model δ_c shows that the phase changes suffered by electron waves impinging on the metal surface are not as extreme as those required by a sharp join of image and interior potentials. Some of the difference may lie in the use of the WKB approximation just to the right of x_1 (Fig. 1). Since δ_x is essentially the same for all three metals studied, the actual form of the surface potential should be similar for tungsten, tantalum, and molybdenum.

Deviation amplitudes depend strongly on the form of the potential at the barrier maximum, a difficulty which does not appear to be shared by the phase. As a result, the computation of $|\mu|$ from the experimental amplitudes, using a theoretical expression founded on a parabolic potential at x_0 , has little merit except in providing an order of magnitude check on the box model values and an indication that the parabolic form is not completely satisfactory.¹⁵ Further refinements could be made in the calculation of the energy-dependent phase of the unaveraged periodic transmission coefficient [see Eq. (12)], and in the averaging of this coefficient, but it is doubtful whether such improvement in method would yield any essential change in the amplitude.

Theoretically, it should be of interest to discover what type of potential at the surface is necessary to reduce the phase change at this point by a quarter period. Also, it should be advantageous to adjust present approximations to the extent that $|\mu|$, which is important in emission phenomena other than thermionic, may be computed with some degree of accuracy from experimental deviation amplitudes. Experimentally, it is important that the analysis embodied in Tables I and II be repeated for data taken on single crystals and contaminated metallic surfaces, in order to ascertain the sensitivity of the periodic deviation effect as a device for investigating surface conditions.

The authors acknowledge the assistance of Drs. C. Herring and C. J. Mullin, whose suggestions were valuable in completing this work.

¹⁵ Work now being carried on by C. J. Mullin and G. S. Colladay indicates that this deficiency may be rectified by the use of a cubic approximation to the mirror-image potential near the barrier top.